RESEARCH ARTICLE
doi: 10.2306/scienceasia1513-1874.2021.061

ScienceAsia 47 (2021): **506–513**

Modified phoenix tree leaves and their adsorption removal of Ca^{2+} from wastewater

Sen Wang[a,b,*], **TianLong Li**[a], **Pei Yi**[a], **JiaoJiao Yuan**[a]

[a] School of Environmental Science and Engineering, Shaanxi University of Science and Technology, Xi'an 710021 China

[b] National Demonstration Center for Experimental Light Chemistry Engineering Education (Shaanxi University of Science & Technology), Xi'an 710021 China

[*]Corresponding author, e-mail: wangsen@sust.edu.cn

Received 10 Dec 2020
Accepted 25 Apr 2021

ABSTRACT: Too much Ca^{2+} in the water would have a bad effect on the papermaking process. Phoenix tree leaves were modified by NaOH or H_3PO_4 treatment for Ca^{2+} adsorption and characterized by X-ray diffraction (XRD), scanning electron microscopy (SEM), and Fourier transform infrared spectroscopy (FTIR). The effects of adsorption time, particle size, and adsorbent dosage on Ca^{2+} adsorption from wastewater were studied. Moreover, the adsorption kinetics and thermodynamics of Ca^{2+} adsorption before and after modification were analyzed. Results showed that the surface of natural phoenix tree leaves is relatively smooth without obvious porosities prior to modification. After modification, the surface of the leaves became loose and rough; and concave pores were also found. After NaOH-modification, functional groups on the surface of the phoenix tree leaves increased, which is conducive to adsorption. The removal effect of Ca^{2+} by NaOH-modified leaf adsorbent was better than that by H_3PO_4. Under optimal conditions, the NaOH-modified phoenix tree leaves had a removal efficiency of 74.18% for Ca^{2+} in the wastewater. The adsorption process was consistent with the pseudo-second-order kinetic reaction and Langmuir isotherm equations.

KEYWORDS: adsorbent, Ca^{2+}, modified phoenix tree leaves, papermaking wastewater

INTRODUCTION

Paper industry is one of the industries with high energy and material consumption and environmental pollution concern. The pollution problem in the paper industry is very serious and has attracted wide attention. At present, emissions of wastewater in paper industry and COD in various industries accounted for the dominant position in environmental pollution. A large amount of wastewater with high concentration of inorganic pollutants is produced because of extensive water consumption in the paper industry. Pollutants, especially those in wastewater, are likely to cause serious damage to the environment [1]. Metal ions, such as Na^+, Cu^{2+}, Fe^{3+}, Mn^{2+}, Al^{3+}, and Ca^{2+} can be found in wastewater in different concentrations; while some ions, such as Ca^{2+}, combine with CO_3^{2-}, S^{2-}, SiO_3^{2-}, and other anions and form sediments [2]. The Ca^{2+} in wastewater mainly comes from [3]: (1) raw materials, including a small amount of recycled wastepaper; (2) additives containing Ca^{2+}, such as $CaCO_3$ fillers, which could remain in paper and water; (3) pollutant accumulation caused by the increased use of recycled papermaking. The concentration of Ca^{2+} in pulping and papermaking wastewater is rather high, about 1000 mg/l. If not handled properly, the wastewater Ca^{2+} can cause not only scaling on production equipment and pipelines, but also sludge calcification in biological wastewater treatment reactors [4]. At present, papermaking wastewater treatment processes mainly include precipitation, advanced oxidation, membrane separation, and adsorption methods. In this study, modified phoenix tree leaves were used as Ca^{2+} adsorbent in papermaking wastewater, an advantage of regeneration and pollution-free accord with the general trend of contemporary environmental governance.

Biosorption of toxic contaminants, such as heavy metals and high level of ions from industrial and sewage wastewater, using microorganisms and agricultural wastes has been a method of choice for environmental cleanup [5]. Agricultural wastes mainly refer to food crop waste, leaves, and wood waste, composed of lignin, cellulose, and hemicellulose; which are porous, with a large specific surface area and a wide range of sources, and water

insoluble, Phoenix is a widely planted greening tree species in northern China. It produces a large number of leaves in winter each year, and the leaves are basically treated as garbage, contributing to not only environmental pollution, but also great waste of resources. Studies have shown that modified phoenix tree leaves, a type of natural waste, can be used as a biomass resource to adsorb pollutants form wastewater due to its rich lignin and cellulose contents [6], and they have been used as adsorbents to remove Ca^{2+} from papermaking wastewater. Using modified phoenix tree leaves not only saves on the cost of sewage treatment, which presents great practical significance to the papermaking industry, but also recycles common waste in wastewater and helps control and prevent environmental deterioration [7]. Moreover, modified phoenix tree leaves kept in the sewage treatment are in powder form, which will eventually be transformed into sludge and discharged, increasing the organic composition of sludge and facilitating the operation of sludge composting.

In the present study, the adsorption of Ca^{2+} in papermaking wastewater by H_3PO_4- and NaOH-modified phoenix tree leaves was investigated. The leaves were subjected to X-ray (XRD), scanning electron microscopy (SEM), and Fourier transform infrared spectroscopy (FTIR) before and after modification. The results of the study provided a scientific basis supporting the use of phoenix tree leaves for wastewater treatment.

MATERIALS AND METHODS

Materials, chemical reagents, and apparatus

The phoenix tree leaves were collected within the campus, and wastewater was prepared in the laboratory according to the wastewater indices of a papermaking wastewater treatment plant. The water characteristics are as follows: pH 6.93–7.98, COD_{Cr} 2360–3782 mg/l, Ca^{2+} concentration 850–1400 mg/l, and conductivity 2327–3208 μS/cm. Deionized water was obtained from a Millipore Alpha Q-Waters purification system (Billerica, MA, USA). NaOH, H_3PO_4, HNO_3, and $CaCl_2$ were purchased from Shanghai Chemical Pharmaceutical Company (China).

The apparatus used in this study included a constant temperature shaking bed (HZP-91,Shanghai Liangyi Scientific Instrument Co., Ltd., China), an X-ray diffraction analyzer (D8 ADVANCE, Brooke (Beijing) Technology Co., Ltd., Germany), an ICP-AES workstation (ICAP 6300, Thermo Fisher Technology Co., Ltd., USA), an environmental scanning electron microscope (FEI Q45, Tisken Trading (Shanghai) Co., Ltd., China), and a circulating water multi-purpose vacuum pump (SHB-3, Zhengzhou Dufu Instrument Factory, China).

Preparation of phoenix tree leaf powder

The pretreated phoenix tree leaves were baked for 24 h at 60 °C in an oven until a constant weight was achieved. Thereafter, the leaves were powdered and sifted through a series of different sizes of sieves: 20–40 mesh, 60–80 mesh, and 100 mesh.

Preparation of modified phoenix tree leaves

Exactly 10 g of each size of phoenix tree leaf powders was placed in separate 500 ml Erlenmeyer flasks. Then, 1% (w/w) NaOH or H_3PO_4 solution (200 ml) was added to each flask, and the resulting mixtures were shaken in a constant temperature oscillator at room temperature for 720 min. After filtration, the residue was washed to neutral pH and then baked at 60 °C in an oven to a constant weight.

Characterization

The isoelectric point [8], surface morphology [9], and functional groups and characteristic peaks of natural and modified phoenix tree leaves were characterized via isoelectric point measurements [10], FTIR, SEM, and XRD, respectively.

Effects of size and dose of adsorbents and incubation time on Ca^{2+} adsorption

The solution pH of the modified adsorbents, 60–80 mesh NaOH-modified and 100-mesh H_3PO_4-modified (or 20–40, 60–80, and 100 mesh size if size was varied) applied at a dosage of 12 g/l (or 3–13 g/l if dose was varied) was adjusted to neutral, and 50 ml of Ca^{2+} solution with an initial concentration of 1 g/l was added. The mixtures were then shaken at 25 °C, 150 rpm for 120 min (or 30–240 min if time was varied). After that, the mixture was filtered, and the removal efficiencies of Ca^{2+} were calculated according to Eq. (1). All analyses were performed in triplicate and accompanied by corresponding blank controls.

Ca^{2+} removal efficiency

The Ca^{2+} concentration was determined via ICP-AES [11], and the Ca^{2+} removal efficiency of the adsorbent was calculated by the following equation [12]:

$$\eta = \frac{C_0 - C}{C_0} \times 100\% \quad (1)$$

where η is the Ca^{2+} removal efficiency; C_0 (mg/l) the initial Ca^{2+} concentration; and C (mg/l) the remaining Ca^{2+} concentration after adsorption.

Adsorption kinetic model

Here the influence of various factors on the adsorption process was studied [13]. The modified adsorbents (12 g/l) were added to Ca^{2+} solution (initial concentration of 1 g/l), and the solution pH was adjusted to neutral. The mixtures were then shaken at 150 rpm at 25, 40, or 55 °C for 30, 60, 90, 120, 180, or 240 min. After filtration, Ca^{2+} remained in the solution was calculated. The linear expression of the pseudo-second-order kinetic equation is according to Eq. (2) [14]:

$$\frac{t}{q_t} = \frac{1}{k_2 {q_e}^2} + \frac{t}{q_e} \tag{2}$$

where q_t is the adsorption amount (mg/g) at time t, q_e is the adsorption amount at adsorption equilibrium (mg/g), and k_2 is the pseudo-second-order adsorption rate constant.

Isothermal adsorption model

The solution pH of the 60–80 mesh NaOH- and H_3PO_4-modified adsorbents (at 12 g/l) was adjusted to neutral, and 100 ml of Ca^{2+} solution with initial concentrations of 0.1, 0.3, 0.5, 0.7, 0.9, or 1 g/l were added. The mixtures were then shaken at 25 °C and 150 rpm for 2 h, and then filtered to determine the Ca^{2+} concentrations remaining in the filtrates.

The Langmuir isotherm [15, 16] is a theoretical equation commonly used to analyzed solid adsorption; and the equation assumes that adsorption occurs on a plane containing the adsorption point of solids. Each adsorption point can only accommodate one molecule; adsorption is reversible, and its mathematical expression is as follows:

$$q_e = \frac{Q^0 C_e}{(b + C_e)} \tag{3}$$

where q_e is the adsorption amount (mg/g) at adsorption equilibrium, Q^0 is the saturated adsorption amount (mg/g), which visually characterizes the adsorption capacity of the adsorbent for the adsorbate, and b is the equilibrium constant of adsorption. Note that, at a certain temperature, Q^0 and b are constant for a certain adsorbent and adsorbate. After the linearization of Eq. (3): $1/q_e = 1/Q^0 + (b/Q^0)(1/C_e)$, and $1/q_e$ is plotted against $1/C_e$ to obtain each eigenvalue.

RESULTS AND DISCUSSION

Isoelectric point of the adsorbent

Natural, NaOH-, and H_3PO_4-modified phoenix tree leaf adsorbents were determined (Fig. 1). The isoelectric points of the adsorbent before and after NaOH modification were 5.6 and 6.1, respectively. The results indicated that alkali functional groups on the surface of the adsorbents increased after the modification [17]. The pH of the external solution of the NaOH-modified adsorbent was higher than 6.1, and the negative charge on the adsorbent surface was favorable for adsorbing cations [18]. For H_3PO_4-modification, the isoelectric point of the modified adsorbent was decreased to 5.1, indicating that the H_3PO_4-modified adsorbent had fewer alkaline functional groups and slightly more acid functional groups on its surface compared with those of the NaOH-modified adsorbents. Thus, cation adsorption effect of the H_3PO_4-modified adsorbent may be weak when the pH of the external solution is greater than 5.1.

Fourier transformed infrared spectrometric analysis

FTIR was used to analyze the functional groups of tree leaf adsorbents (Fig. 2). The strong absorption peak at 3323.12 cm^{-1} reflects the associated alcohol or stretching vibrations peak of —OH in phenol. The peak at 2922.12 cm^{-1} is caused by the asymmetric stretching vibrations of saturated C—H bonds, and the weak peak at 2849.68 cm^{-1} is due to the symmetric stretching vibrations of C—H bonds. The characteristic absorption peaks of C=O in the carboxylic acid and ketone appear at 1727.89 cm^{-1} and 1673.01 cm^{-1}, respectively. The peak at 1408.84 cm^{-1} corresponds to the bending vibrations of O—H, and the peak at 1335.67 cm^{-1} reflects the asymmetric bending vibrations of C—H. The peak at 1300–1100 cm^{-1} indicates the stretching vibrations of C—O in carboxylic acid or ethanol. The peak of 1043.70 cm^{-1} reflects the C—O stretching vibrations of alcohol. In summary, a large number of carboxyl and hydroxyl groups may be found on the surface of natural phoenix tree leaves. After NaOH modification, the stretching peak of —OH and the characteristic absorption peak of C=O showed a red shift, and the intensity of the peak was significantly weakened; these phenomena indicated that some components were dissolved after modification.

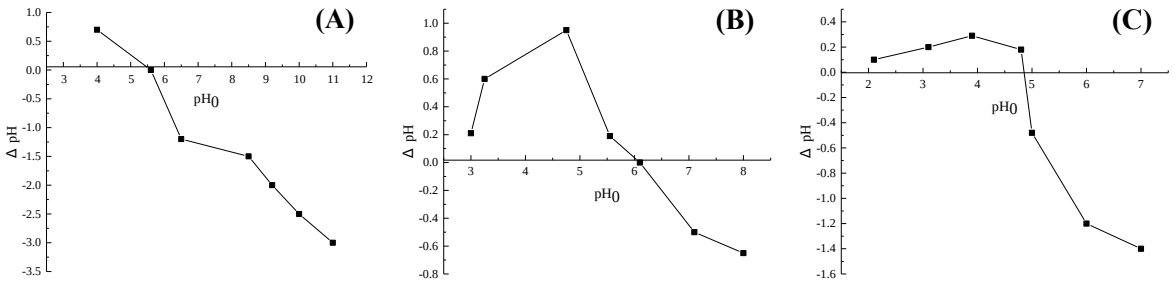

Fig. 1 Isoelectric points of leaf adsorbents: (A) natural, (B) NaOH-modified, and (C) H_3PO_4-modified.

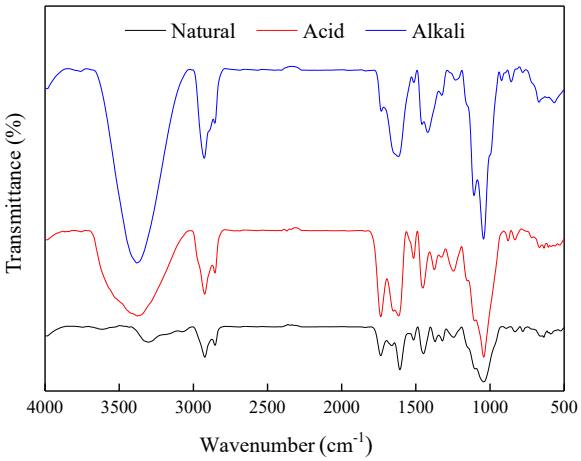

Fig. 2 Diagram of the natural and modified leaf adsorbents.

X-ray diffraction analysis

XRD was used to analyze the crystal structures of the natural and modified leaf adsorbents (Fig. S1). Although the diffraction peak intensities of the natural, NaOH-modified, and H_3PO_4-modified adsorbents showed some variations, the positions of three main peaks and most secondary peaks showed little difference. A secondary peak at around 15° and a dominant peak near 21° were observed; these two peaks are consistent with those in the XRD diagram of natural cellulose materials [19]. The secondary peak at around 15° reveals a low-order polysaccharide structure. The dominant peak near 21° indicates the crystal structure of cellulose. The peak intensities of the modified adsorbents, which were between 5° and 80°, were higher than that of those of the natural adsorbent, thus indicating that the structure of the phoenix tree leaves evolved in a regular and orderly manner after modification [20].

Appearance and morphological analysis

The adsorbents' SEM results are shown in Fig. 3. It can be seen that the surface of the natural leaf adsorbent was relatively smooth, and no obvious porosity could be observed. By comparison, the surface of the modified leaf adsorbents was loose and rough; and concave pores were also found. Compared with that of H_3PO_4-modified leaves, the surface of NaOH-modified leaves was looser and larger; and it also showed a honeycomb shape, which could expose more adsorption sites and be conducive to adsorption. Alkali treatment may lead to internal fractures within the hydrogen bonds of the adsorbents. OH^- groups react violently with the cellulose and hemicellulose of the leaf powders, and the original structure is destroyed, thereby forming a complex layered structure [21]. The chlorophyll of the leaf surface and some light-molecular weight compounds are simultaneously removed, and active groups were exposed, which increases the opportunity of the metal ion actions.

Effects of H_3PO_4- and NaOH-modified leaf adsorbents on Ca^{2+} adsorption

The removal efficiencies of the modified leaf adsorbents were significantly higher than those of the natural adsorbents. When the same amount of adsorbent was added to the adsorption process, the Ca^{2+} removal efficiency of the NaOH-modified adsorbent was significantly higher than that of the H_3PO_4 modified adsorbent (Fig. 4).

Effects of adsorbent's particle sizes on Ca^{2+} adsorption

Fig. 5 shows the Ca^{2+} removal effects as a function of adsorbent particle size. When the adsorption time was 120 min and the applied dosage of adsorbent was 12 g/l, the Ca^{2+} removal efficiency of the 60–80 mesh (optimal size) NaOH-modified adsorbent was 74.18%, by comparison, the Ca^{2+} removal ef-

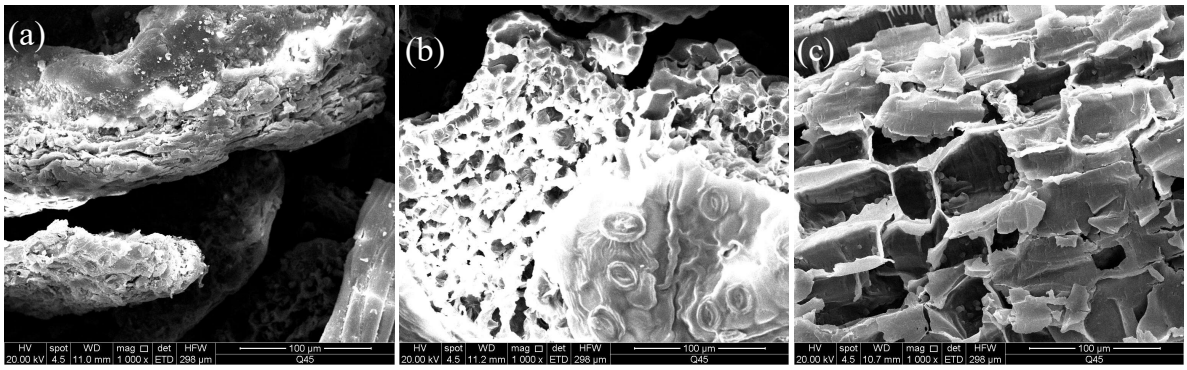

Fig. 3 SEM images of (a) natural, (b) H_3PO_4-modified, and (c) NaOH-modified leaf adsorbents.

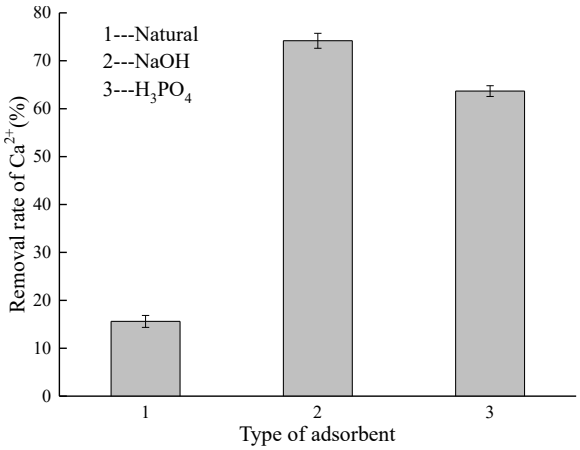

Fig. 4 Ca^{2+} adsorption effects of natural and modified leaf adsorbents.

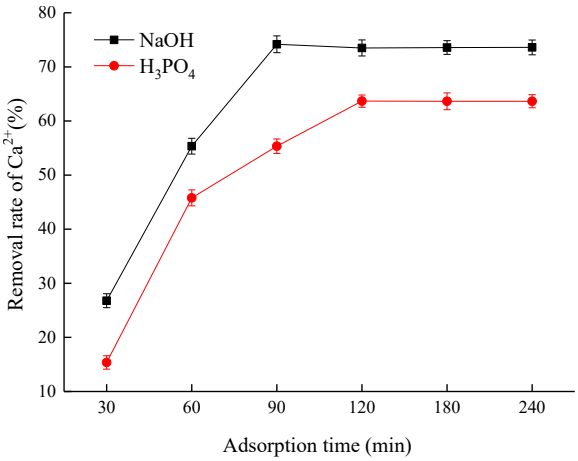

Fig. 6 Ca^{2+} removal effects as a function of adsorption time.

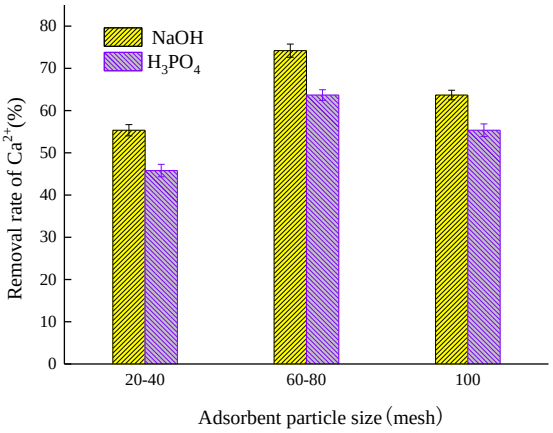

Fig. 5 Ca^{2+} removal effects as a function of adsorbent particle size.

ficiency of the 100-mesh was 65.46%. The performance of the adsorbent improved with decreasing particle size due to the increases in specific surface area and the enhanced availability of adsorption sites [22]. However, in case of NaOH-modified adsorbent, the optimal size was 60–80 mesh. As a strong base, NaOH could damage the surface of the smaller particle size (20–40 mesh) resulting in the reduction of adsorption sites and the decrease of Ca^{2+} removal [23]. Moreover, the Ca^{2+} removal effect of the NaOH-modified adsorbents was significantly better than that of the H_3PO_4-modified leaves.

Effects of time on Ca^{2+} adsorption

Fig. 6 shows the Ca^{2+} removal effects as a function of adsorption time. The maximum Ca^{2+} removal efficiency of the NaOH-modified adsorbent was 74.18%, and the adsorption equilibrium was reduced after 90 min. The maximum Ca^{2+} removal efficiency of the H_3PO_4-modified adsorbent was 63.67%, and adsorption equilibrium was reached

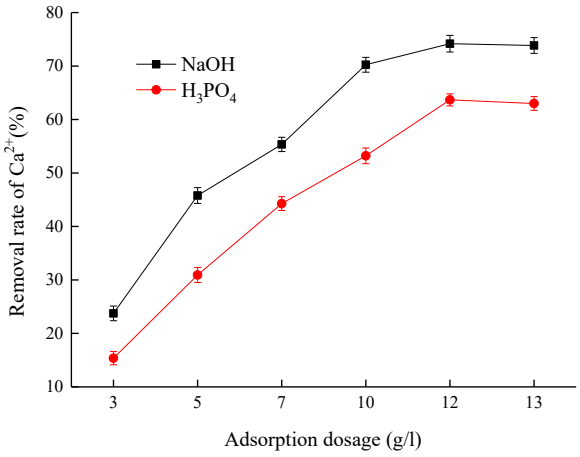

Fig. 7 Ca^{2+} removal effects as a function of adsorption dosage.

after 120 min. No Ca^{2+} adsorption by both adsorbents was observed after the adsorption equilibrium was reached, likely because leaves contain cellulose, hemicellulose, proteins, amides, and other carbohydrates, with hydroxyl, carboxyl, and other active groups capable of forming coordination complex with metal ions [24]. At the initial stage of the reaction, Ca^{2+} was rapidly adsorbed. As the reaction time increased, binding sites on the adsorbent surface and the binding and exchange of ions in the solution tended to become saturated, and the adsorption rate gradually slowed down [25]. At adsorption equilibrium, the adsorption rate fluctuated, and desorption might occur due to excessive shaking time [26].

Effects of adsorbent dosage on Ca^{2+} adsorption

The results showed in Fig. 7 indicated that the same Ca^{2+} adsorption trend and equilibrium were achieved by both adsorbents at a dosage of 12 g/l. In this experiment, incubation time for NaOH-modified adsorbent was 90 min while that for H_3PO_4-modified was 120 min. The Ca^{2+} removal efficiency increased significantly at the initial stage of adsorption but, then. slowed down with increasing adsorbent dosage. These results indicate that high Ca^{2+} adsorption rates occurred at low proportion of the modified leaf adsorbent. With the same dosage, the Ca^{2+} removal efficiency of the NaOH-modified adsorbents was significantly higher than that of H_3PO_4-modified leaves. At the same initial Ca^{2+} concentration, Ca^{2+} adsorption decreased with increasing dosage of the unit mass of modified leaf adsorbent because increased amount of available adsorbent increased the specific surface area and corresponding adsorption sites, thereby leading to a decrease in adsorption capacity of the unit mass [27, 28].

Adsorption and verification experiments of industrial wastewater

The Ca^{2+} concentration in the papermaking plant wastewater was originally 938 mg/l. When the NaOH-modified leaves (60–80 mesh) were applied as follows: adsorbent concentration, 12 g/l; temperature, 25 °C; solution pH, 7; and adsorption time, 90 min; the Ca^{2+} concentration in the wastewater dropped to 279.5 mg/l, which translates to a removal efficiency of 70.2%.

The results in Table 1 indicated that the adsorbents presented certain removal effects on both COD_{Cr} and Ca^{2+}. However, the adsorption effect did not reach the maximum, especially for the removal of Ca^{2+}. It is likely that there are a large number of other metal ions and organic pollutants in the actual wastewater, which inevitably affect the adsorption capacity of the adsorbent and occupy the adsorption sites. As a result, Ca^{2+} could not be effectively adsorbed, and the Ca^{2+} adsorption effect of the adsorbent was limited.

Adsorption kinetic model

Adsorption kinetics is an important parameter in the design of adsorption systems. Fig. S2 shows the fitting curve of the pseudo-second-order kinetic equation. The R^2 of the linear regression coefficient exceeded 0.98, which means the data fit the pseudo-second-order adsorption kinetic equation well. These findings indicate the occurrence of a chemical action during the absorption process. Adsorption is a control step during Ca^{2+} removal by the modified phoenix tree leaves [29]. The equilibrium adsorption amount and the adsorption rate of the NaOH-modified leaf adsorbent were higher than those of the H_3PO_4-modified adsorbent.

Isothermal adsorption model

The results indicated that the adsorption rate first increased and then stabilized with increasing initial concentration, and the adsorption capacity of the system increased gradually. The maximum adsorption rate and adsorption capacity were 74.18% and 59.87 mg/g, respectively. Fig. S3 shows the fitting curve of the Langmuir adsorption isotherm. The R^2 values of the NaOH- and H_3PO_4-modified adsorbents were 0.8498 and 0.7617, respectively, indicating a good fit.

Table 1 Water quality indicators before and after adsorption.

Treatment	pH	COD_{Cr} (mg/l)	Ca^{2+} (mg/l)	Conductivity (μS/cm)
Non-treated water	7.56 ± 0.68	2817 ± 75	915.6 ± 40	3215 ± 122
Treated water	7.12 ± 0.52	2103 ± 72	272.9 ± 58	186 ± 93.5
Ca^{2+} removal efficiency (%)	–	–	70.2 ± 4.8	–

Index values in the table reflect average values.

CONCLUSION

Comparison and analysis of the XRD, SEM and FTIR characteristics of the phoenix tree leaves before and after modification revealed increase in the negative potentials of the modified leaves and a larger specific surface area. Moreover, the modified adsorbents showed a looser and rougher texture, which is conducive to Ca^{2+} adsorption from wastewater. FTIR showed that the functional groups of the modified leaves could promote adsorption. The adsorption effects of modified leaves on Ca^{2+} was significantly better than that of natural leaves, and leaf adsorbents modified by NaOH had better effects on Ca^{2+} removal than those modified by H_3PO_4. Under optimal conditions, the Ca^{2+} removal efficiency of the NaOH-modified adsorbent (74.18%) was much higher than that of the H_3PO_4-modified (63.67%). Ca^{2+} adsorption from wastewater by NaOH-modified leaves is consistent with the Langmuir adsorption isotherm and pseudo-second-order kinetic reaction equations.

Appendix A. Supplementary data

Supplementary data associated with this article can be found at http://dx.doi.org/10.2306/scienceasia1513-1874.2021.061.

Acknowledgements: The authors would like to express heartfelt thanks to the financial support from Shaanxi Science and Technology Plan Project(2018SF-377), Technical Innovation Guidance Project of Shaanxi Province(2019CGXNG-039), and the Project of National Demonstration Center for Experimental Light Chemistry Engineering Education(Shaanxi University of Science & Technology)(2018QGSJ02-04).

REFERENCES

1. Chen DZ (2018) Development status and trend of pulping and papermaking wastewater treatment. *Chem Ind Yunnan* **45**, 177–178.
2. Li RH, Gao BY, Guo KY, Yue QY (2017) Effects of papermaking sludge-based polymer on coagulation behavior in the disperse and reactive dyes wastewater treatment. *Bioresour Technol* **23**, 59–67.
3. Zhou YT, Zhao H, Bai HL, Zhang LP (2012) Papermaking effluent treatment: A new cellulose nanocrystalline/polysulfone composite membrane. *Procedia Environ Sci* **16**, 145–151.
4. Van LEPA, Van AA, Van LJB, Hamelers HVM, Lettinga G, Gonzalez-Gil G (1998) Effects of high calcium concentrations on the development of methanogenic sludge in upflow anaerobic sludge bed (UASB) reactors. *Water Res* **32**, 1255–1263.
5. Al-Hagar EAO, Bayoumi RA, Aziz OAA, Mousa AM (2020) Biosorption and adsorption of some heavy metals by *Fusarium* sp. F6c isolate as affected by gamma irradiation and agricultural wastes. *ScienceAsia* **46**, 37–45.
6. Ren XF, Han RP (2014) Study of adsorption of typical dyes and 2,4-dichlorphenol from aqueous solution by modified phoenix tree leaf. Master thesis, Zhengzhou Univ, China.
7. Lv CF, Wang J, Gao PP (2014) Study on preparation and properties of activated carbon from Chinese parasol leaves by phosphoric acid-microwave method. *Appl Chem Ind* **43**, 824–826.
8. Hsieh HS, Pignatello JJ (2018) Modified carbons for enhanced nucleophilic substitution reactions of adsorbed methyl bromide. *Appl Catal B* **233**, 281–288.
9. Chen JP, Wang LY, Su XJ (2016) Structure, morphology, thermostability and irradiation-mediated degradation fractions of hemicellulose treated with gamma-irradiation. *Waste Biomass Valori* **7**, 1415–1425.
10. Aliakbari Z, Younesi H, Ghoreyshi AA (2018) Production and characterization of sewage-sludge based activated carbons under different post-activation conditions. *Waste Biomass Valori* **9**, 451–463.
11. Castro PS, Bertotti M, Naves AF (2017) Hybrid magnetic scaffolds: The role of scaffolds charge on the cell proliferation and Ca^{2+} ions permeation. *Colloid Surface B* **56**, 388–396.
12. van Langerak EPA, Ramaekers H, Wiechers J, Veeken AHM, Hamelers HVM, Lettinga G (2000) Impact of location of $CaCO_3$ precipitation on the development of intact anaerobic sludge. *Water Res* **34**, 437–446.
13. He YH, Lin H, Dong YB, Wang L (2017) Preferable adsorption of phosphate using lanthanum-incorporated porous zeolite: Characteristics and mechanism. *Appl Surf Sci* **426**, 995–1004.

14. Gunasundari E, Kumar P (2017) Adsorption isotherm, kinetics and thermodynamic analysis of Cu(II) ions onto the dried algal biomass (*Spirulina platensis*). *J Ind Eng Chem* **56**, 129–144.
15. Chakravarty S, Mohanty A, Sudha TN, Upadhyay AK, Konar J, Sircar JK, Madhukar A, Gupta KK (2010) Removal of Pb(II) ions from aqueous solution by adsorption using bael leaves (*Aegle marmelos*). *J Hazard Mater* **173**, 502–509.
16. Mashitah MD, Yus Azila Y, Bhatia S (2008) Biosorption of cadmium(II) ions by immobilized cells of *Pycnoporus sanguineus* from aqueous solution. *Bioresour Technol* **99**, 4742–4748.
17. Shen J, Wang XZ, Zhang Z (2017) Adsorption and degradation of C-14-bisphenol A in a soil trench. *Sci Total Environ* **607**, 676–682.
18. Molatlhegi O, Alagha L (2017) Adsorption characteristics of chitosan grafted copolymer on kaolin. *Appl Clay Sci* **150**, 342–353.
19. Yan B, Niu CH, Wang J (2017) Kinetics, electron-donor-acceptor interactions, and site energy distribution analyses of norfloxacin adsorption on pretreated barley straw. *Chem Eng J* **330**, 1211–1221.
20. Gao YX, Yu G, Liu K, Deng SB, Wang B (2017) Integrated adsorption and visible-light photodegradation of aqueous clofibric acid and carbamazepine by a Fe-based metal-organic framework. *Chem Eng J* **330**, 157–165.
21. Briao GV, Jahn SL, Foletto EL, Dotto GL (2017) Adsorption of crystal violet dye onto a mesoporous ZSM-5 zeolite synthetized using chitin as template. *J Colloid Interface Sci* **508**, 313–322.
22. Liu B, Gu J, Tu YY (2014) Adsorption of different polar phenolic substances by activated carbon from phoenix tree leaves. *Res Environ Sci* **27**, 92–98.
23. Nie XQ, Dong FQ, Liu MX (2013) Adsorption behavior of biosorbent eucalyptus leaves on uranium. *Spectrosc Spect Anal* **33**, 1290–1294.
24. Fu J, Song R, Mao WJ (2011) Adsorption of disperse blue 2BLN by microwave activated red mud. *Environ Prog Sustain* **30**, 558–566.
25. Zheng XY, Xu SP, Wang Y (2018) Enhanced degradation of ciprofloxacin by graphitized mesoporous carbon (GMC)-TiO_2 nanocomposite: Strong synergy of adsorption-photocatalysis and antibiotics degradation mechanism. *J Colloid Interface Sci* **527**, 202–213.
26. Ali A, Gul A, Mannan A (2018) Efficient metal adsorption and microbial reduction from Rawal Lake wastewater using metal nanoparticle coated cotton. *Sci Total Environ* **639**, 26–39.
27. He JY, Li YL, Wang CM (2017) Rapid adsorption of Pb, Cu and Cd from aqueous solutions by beta-cyclodextrin polymers. *Appl Surf Sci* **426**, 29–39.
28. Lei CS, Pi M, Xu DF, Jiang CJ (2017) Fabrication of hierarchical porous ZnO-Al_2O_3 microspheres with enhanced adsorption performance. *Appl Surf Sci* **426**, 360–368.
29. Ren G, Wang X, Huang P, Zhong B (2017) Chromium(VI) adsorption from wastewater using porous magnetite nanoparticles prepared from titanium residue by a novel solid-phase reduction method. *Sci Total Environ* **607**, 900–910.

Appendix A. Supplementary data

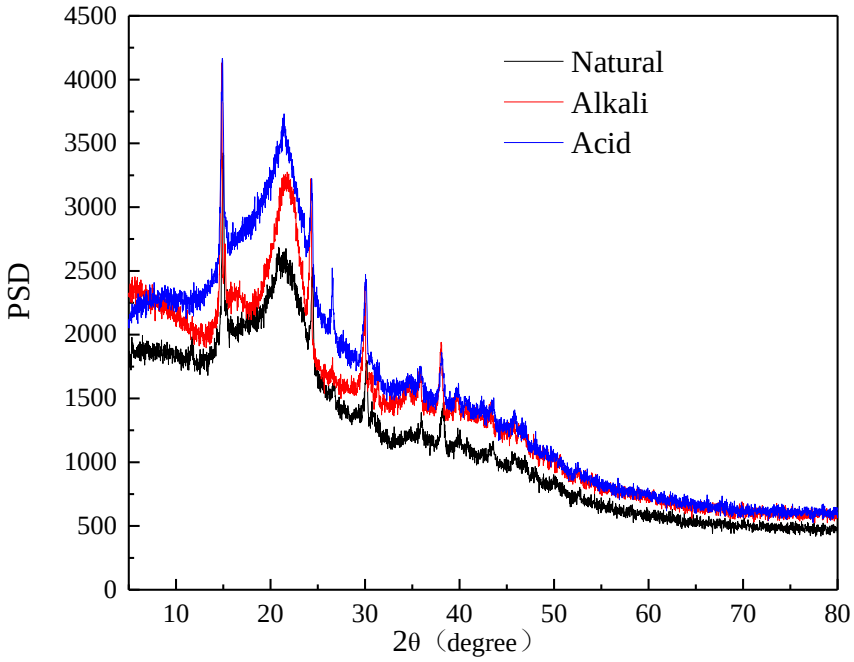

Fig. S1 XRD patterns of the natural and the modified phoenix tree leaf adsorbents.

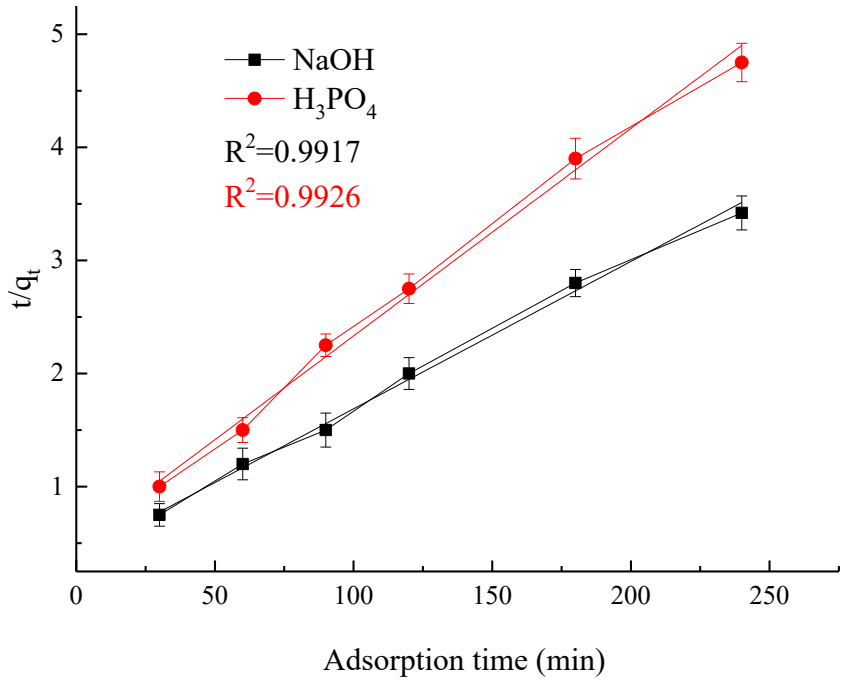

Fig. S2 Fitting curve of pseudo-second-order kinetic equation of adsorption.

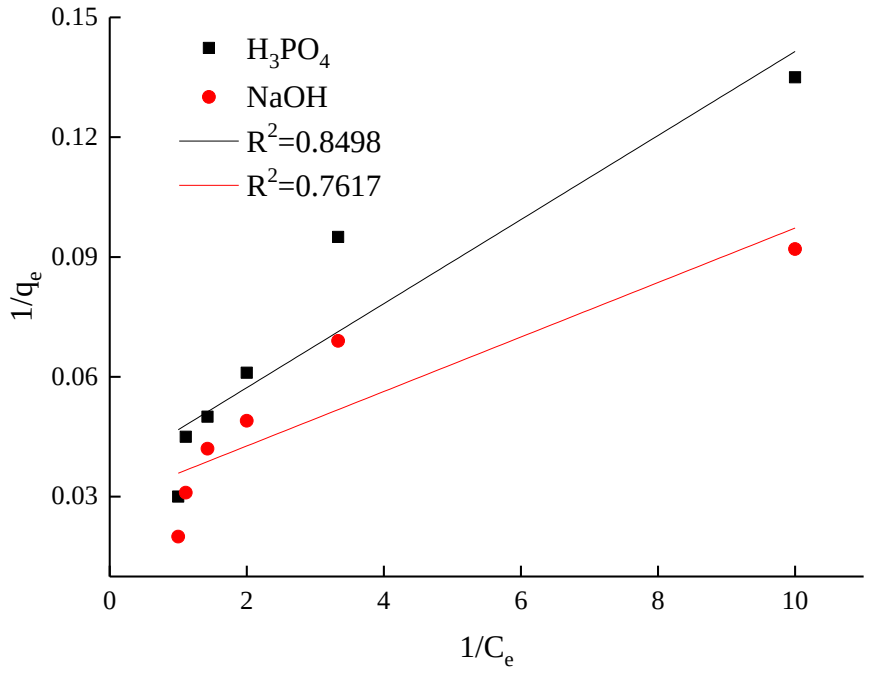

Fig. S3 Fitting curve of the Langmuir adsorption isotherm.